$O_u^+(^3\Pi_u)\leftarrow XO_g^+(^1\Sigma_g^+)$ transitions in Zn_2 excited in crossed molecular and laser beams

M. Czajkowski, R. Bobkowski,* and L. Krause
Department of Physics, University of Windsor, Windsor, Ontario, Canada N9B 3P4
and Ontario Laser and Lightwave Research Centre, Windsor, Ontario, Canada N9B 3P4
(Received 14 August 1989)

The $O_u^+(^3\Pi_u)\leftarrow XO_g^+(^1\Sigma_g^+)$ excitation spectrum of Zn_2 van der Waals molecules produced in a molecular beam employing free-jet supersonic expansion, crossed with a pulsed dye-laser beam, was studied using Ar as the carrier gas. A well-resolved structure arising from transitions between the vibrational levels of the lower and upper states was recorded at various carrier gas pressures. An analysis of the spectrum yielded the vibrational constants, bond strengths, and equilibrium internuclear separations of the molecule in the two electronic states.

I. INTRODUCTION

Spectroscopic studies of van der Waals and excimer molecules such as Hg_2,[1,2] Cd_2,[3,4] and Zn_2,[5] which are of continuing fundamental interest, are also relevant to the possible development of new excimer lasers.[6] Gas-phase spectroscopy of these molecules presents considerable experimental difficulties because of the relatively low concentrations of the dimers in the atomic vapors, particularly in the cases of Cd_2 and Zn_2. This makes it necessary to carry out experiments at high temperatures which adversely affect the signal-to-noise ratios and cause the resulting spectra to be unduly complex. There have been recent reports of light-induced fluorescence (LIF) experiments carried out in supersonic expansion beams of metals seeded in noble gases,[2-4,7-10] in which much simpler vibrational (and rotational) structures were observed, belonging to very weakly bound van der Waals molecules.

We report here the first observation of an excitation spectrum of Zn_2, obtained in a supersonic expansion beam crossed with a laser beam, which provided information on the $XO_g^+(^1\Sigma_g^+)$ ground state and the $O_u^-(^3\Pi_u)$ excited state correlated with the Zn $4\,^3P_1$ atomic state.

II. DESCRIPTION OF THE APPARATUS AND EXPERIMENTAL PROCEDURE

Figure 1 shows a schematic diagram of the apparatus used to generate the atomic beam and produce the vibronic excitation spectra. Although the expansion chamber and vacuum system were as described previously,[4] some significant changes were made in the beam source and the excitation and detection systems. Because of the relatively low vapor pressure of zinc (compared with cadmium) and of a much smaller oscillator strength of the $^1S_0$-$^3P_1$ atomic transition, the estimated density of Zn_2 molecules resulting from $^3P_1\leftarrow{}^1S_0$ atomic excitation was also smaller by about two orders of magnitude. In attempting to compensate for this by operating the beam source at a higher temperature (1125 K) we found that the jet nozzle became clogged because of a chemical reaction between zinc and iron in the stainless steel, which produced an alloy of high melting temperature. This problem was overcome by constructing the oven and nozzle of molybdenum, which is inert to zinc.[11]

The supersonic Zn_2 beam which also contained Zn and noble-gas atoms, was crossed with a beam of laser light emitted from a frequency-doubled N_2-laser-pumped dye laser whose grating was scanned by a stepper motor-activated sine drive. As can be seen in Fig. 1, the boxcar integrator, the wave meter, and the laser system were all connected to a PC XT computer which controlled the scanning of the dye laser and collected and stored the data from the boxcar for further analysis. The dye laser was operated with Rhodamine 610 in ethanol. The second harmonic was produced with a potassium dihydrogen phosphate (KDP) crystal and the dye laser was frequency calibrated using the Ne optogalvanic spectrum[12] and a wavelength meter.[13] The emitted fluorescence was observed at right angles to the plane of the crossed beams, passed through a UG5 filter, and focused on the photocathode of an EMR 541-N-03-14 photomultiplier tube whose signal was registered with an EG&G 162/166 boxcar integrator and recorded with an X-Y plotter.

To produce a molecular beam the system was evacuated to a pressure below 1 mtorr, the carrier gas was passed

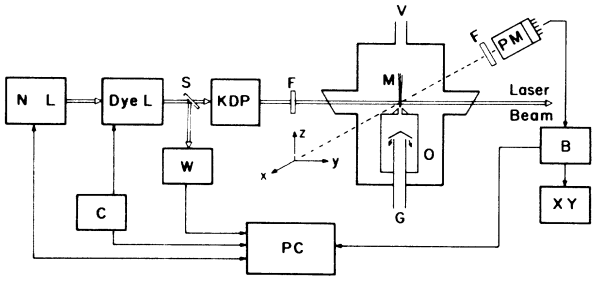

FIG. 1. Schematic layout of the apparatus. O, oven; M, molecular beam; L, lasers; C, scanning controller; W, wavelength meter; B, boxcar integrator; F, filter; G, gas; PM, photomultiplier; V, vacuum line.

through the nozzle ($D=150$ μm) at room temperature, and the oven heating coils were energized; the upper part containing the nozzle was heated first, and then the lower main body. The temperature of the source continued to be raised while maintaining it at 50–80 K above the oven temperature until the operating temperature was reached. A Zn_2 molecular beam was produced at about 900 K, a temperature which was normally reached within 60–90 min. The pulsed laser beam, crossed with the molecular beam, was tuned to a wavelength near the atomic Zn $4\,^4P_1 \leftarrow 4\,^1S_0$ transition and was scanned across the excitation spectrum at the rate of about 1 Å/min.

III. RESULTS AND DISCUSSION

Figure 2 shows a trace of the excitation spectrum of Zn_2 resulting from $O_u^+(^3\Pi_u) \leftarrow XO_g^+(^1\Sigma_g^+)$ vibronic transitions. The assignments of the electronic states are consistent with the potential-energy curves calculated by Bender *et al.*[14] and Hay, Dunning, and Raffenetti.[15] The spectrum, which extends from about 3072 to about 3058 Å, was obtained with argon as the carrier gas at a pressure of 10 atm and with a source temperature of 1000 K. As may be seen in Fig. 2, we continued scanning the spectrum on the long-wavelength side of the Zn $4\,^3P_1 \leftarrow 4\,^1S_0$ atomic line because, at the relatively high carrier-gas pressures used to produce effective cooling, we expected to observe also the ZnAr spectrum arising from the $^3O^+ \leftarrow {}^1O^+$ transitions, similar to the HgAr (Refs. 7 and 10) and CdAr (Refs. 3 and 16) spectra.

Several experiments were performed at various pressures of argon (ranging from 2 to about 12 atm) and at various X/D values[4] ranging from 35 to 70. Simultaneous changes of the carrier-gas pressure and the X/D parameter were necessary to control the terminal Mach number M_T which depends on the gas pressure in the reservoir and the nozzle diameter D:[17]

$$M_T = 133(P_0 D)^{0.4} , \tag{1}$$

where P_0 is the pressure (atm) in the source. The "effective" Mach number is given by

$$M_{\text{eff}} \approx 3.26(X/D)^{0.67} , \tag{2}$$

where X is the distance between the nozzle and the laser beam. M_{eff} should not be smaller than M_T because when $M_T > M_{\text{eff}}$, frequent collisions take place in the supersonic beam causing the appearance of additional "hot bands" and leading to an increased width of the vibrational bands. We observed both phenomena by changing the pressure of the carrier gas in the source. Since the effective Mach number governs also the density n of the atomic species at a point in the beam described by X/D,[17]

$$n = n_0[1+\tfrac{1}{2}(\gamma-1)M_{\text{eff}}^2]^{-1/(\gamma-1)} , \tag{3}$$

where n_0 is the number density in the source and $\gamma = C_p/C_v$, it is impossible to continue elevating the pressure since at high pressures the beam density decreases as M_{eff} increases relative to M_T.

Figure 3 shows the same excitation spectrum as Fig. 2, but obtained at lower X/D and at the same carrier-gas pressure. It is evident from the comparison of Figs. 2 and 3 that the collision frequency affects the intensity of the vibronic band at the long-wavelength end of the spectrum, but the relative intensities of the remaining components of the v' progression appear to be independent of the source temperature or collision frequency. Accordingly, we identified the collision-dependent band as the $v'=0 \leftarrow v''=1$ hot band. The remaining assignments are indicated in Figs. 2 and 3.

Table I lists the measured wavelengths and separations of the vibronic bands in the spectrum and Fig. 4 shows the Birge-Sponer plot of the ΔG values against v', whose intercept yielded the vibrational frequency ω_0' and hence

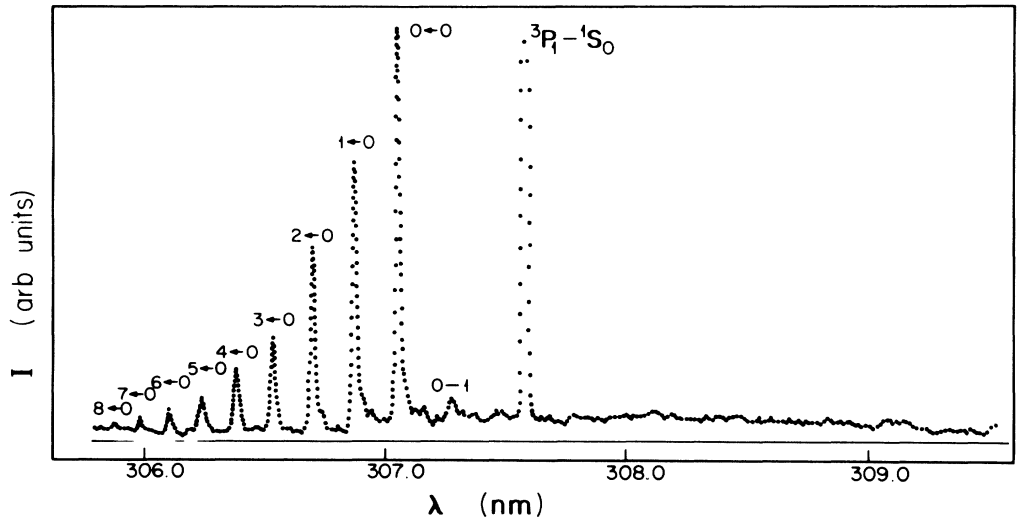

FIG. 2. $O_u^+(^3\Pi_u) \leftarrow XO_g^+\Sigma_g^+)$ excitation spectrum of Zn_2, showing $v' \leftarrow v''$ assignments. The spectrum contains one $0 \leftarrow 1$ "hot band" in addition to the v' progression. Ar was used as the carrier gas.

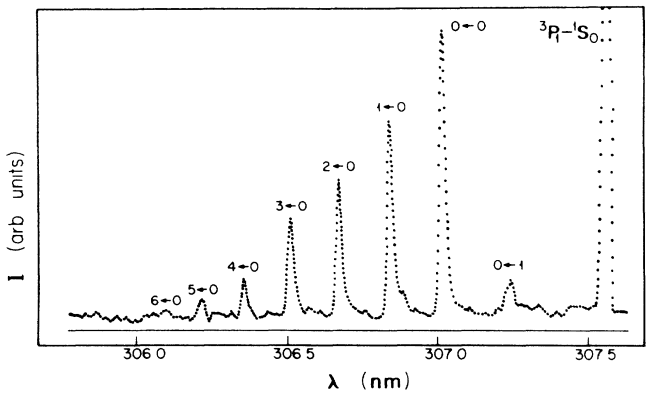

FIG. 3. Zn_2 excitation spectrum produced with a smaller X/D value. Ar was used as the carrier gas. The hot band appears more intense because of enhanced collision frequency.

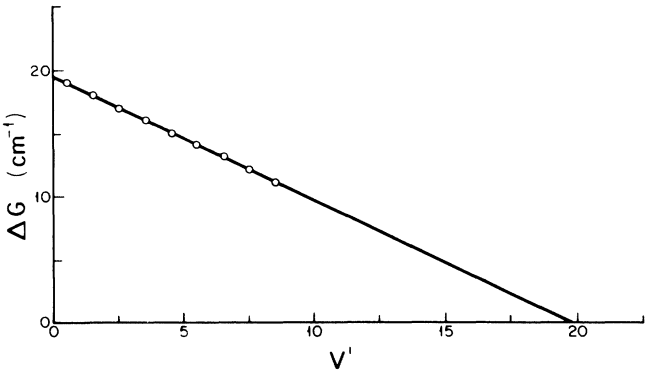

FIG. 4. A Birge-Sponer plot of the v' progression in the Zn_2 spectrum.

the dissociation energy D_0' (and D_e'); the slope produced the anharmonicity $\omega_e x_e$. The straight line was fitted by the method of least squares with the correlation factor of 0.998. The results are listed in Table II, which also includes the parameters for the $XO_g^+(^1\Sigma_g^+)$ ground state calculated from the frequency of the hot band and from the relationship between the dissociation energies of the ground and excited states

$$D_e''[XO_g^+(^1\Sigma_g^+)]=T_e'+D_0'[O_u^+(^3\Pi_u)]-\tilde{\nu}(^3P_1\leftarrow{}^1S_0)\ . \tag{4}$$

No comparison can be made between these results and other experimental or theoretical data since none are available.

TABLE I. Frequencies of vibrational bands observed in the Zn_2 spectrum. The asterisk denotes a hot band.

$v'\leftarrow v''$	$\tilde{\nu}_0$ (cm^{-1})	ΔG (cm^{-1})
0←1	32 533.0*	
		24.3
0←0	32 557.3	
		18.9
1←0	32 576.2	
		18.1
2←0	32 594.3	
		17.0
3←0	32 611.3	
		16.0
4←0	32 627.4	
		15.0
5←0	32 642.4	
		14.0
6←0	32 656.4	
		13.1
7←0	32 669.5	
		12.1
8←0	32 681.6	
		11.0
9←0	32 692.6	

We have also carried out a computer simulation of the excitation spectrum. The Franck-Condon (FC) factors were calculated assuming a Morse potential[18] for the O_u^+ and the XO_g^+ states. The use of the Morse potential appeared to be justified because of the linearity of the Birge-Sponer plot in Fig. 4. We also obtained a very good fit between our experimental Cd_2 spectrum[22] and a computer-simulated spectrum based on the Morse potential. Recent results reported by Fuke *et al.*[7,10] on the HgNe, HgAr, and HgKr van der Waals molecules are also consistent with the respective Morse potentials. These authors carried out a careful (and successful) comparison of the Morse potential with the potential obtained from their experimental data using the Rydberg-Klein-Rees (RKR) method. The simulated spectrum shown in Fig. 5 reproduces faithfully the experimental trace. We found the best fit to be very sensitive to the difference $(r_e'-r_e'')$ where r_e' and r_e'' are the equilibrium internuclear separations in the O_u^+ and XO_g^+ states, respectively. The best fit was obtained for $r_e'-r_e''=0.3\pm0.03$ Å. The red shading of the $O_u^+\leftarrow XO_g^+$ bands indicates that $r_e'(O_u^+)>r_e''(O_g^+)$, which is also evident from the computer simulation. An empirical relation given by Morse for the ground states of homonuclear molecules[18]

$$(r_0'')^3\omega_0''=3000\ \text{Å}^3\,\text{cm}^{-1} \tag{5}$$

leads to rough estimates of r_e' and r_e'', which are also listed in Table II and whose difference $r_e'-r_e''$ agrees with the value obtained from the computer simulation within the stated limits of error. Using the Morse potential[18] and the parameters from Table II, we plotted the potential-energy curves for the XO_g^+ and O_u^+ states which are shown in Fig. 6. We estimate that each of the two potential wells contains 21 vibrational states.

Table III shows the comparison between the spectroscopic constants for the XO_g^+ and O_u^+ states of Hg_2, Cd_2, and Zn_2. The ground-state parameters exhibit a trend which was to be intuitively expected for van der Waals molecules: a decreasing D_e'' and an increasing anharmonicity with decreasing atomic mass, and a decreasing num-

TABLE II. Spectroscopic constants of Zn_2

Designation	$O_u^+(^3\Pi_u)$	$XO_g^+(^1\Sigma_g^+)$[a]
D_0 (cm^{-1})	205±1	261±1
D_e (cm^{-1})	215±1	274±1
ω_0 (cm^{-1})	19.6±0.2	25.1±0.2
ω_e (cm^{-1})	20.1±0.2	25.7±0.2
$\omega_e x_e$ (cm^{-1})	0.47±0.05	0.60±0.05
T_e (cm^{-1})	32 560.4±0.1	
r_e (Å)	5.3±0.07[b], 4.97±0.04[c]	4.80±0.07[b], 4.67[d]
$r_e'-r_e''=0.30\pm0.03$ Å[c]		

[a]Calculated from the "hot band."
[b]Estimated using the Morse approximation.
[c]From the best fit of calculated Franck-Condon factors to the experimental data.
[d]Calculated using the London dispersion relation.

ber of available vibrational levels as the potential well becomes shallower for the less massive molecules. In the O_u^+ states the pattern is similar and even more pronounced. It should be noted that the difference $r_e'-r_e''$ increases with decreasing molecular mass. Unfortunately, no absolute r_e' or r_e'' values are available from spectroscopic data for Cd_2 or Zn_2. A rough theoretical estimate[18] suggests rather large values; $r_e''\simeq4.8$ Å for Zn_2 and 5.1 Å for Cd_2. Recent spectroscopic measurements[2] yielded $r_e''=3.63$ Å and $r_e'=3.61$ Å for Hg_2, though some *ab initio* calculations[2] predicted a larger value $r_e''=4.5$ Å, which is reasonably consistent with our estimates for Cd_2 and Zn_2. We believe that our data have yielded reasonably accurate values of $r_e'-r_e''$. The intensity profiles of the vibrational components clearly indicate that $r_e'>r_e''$; the Hg_2 work indicates, on the other hand, that $r_e'<r_e''$.[2] This apparent, slight inconsistency with the Hg_2 results[12] encouraged us to look at the data shown in Table III from a slightly different point of view. It seemed reasonable to assume that the attractive molecular forces involved in the formation of the Hg_2, Cd_2, or Zn_2 dimers may be characterized by a term of the form

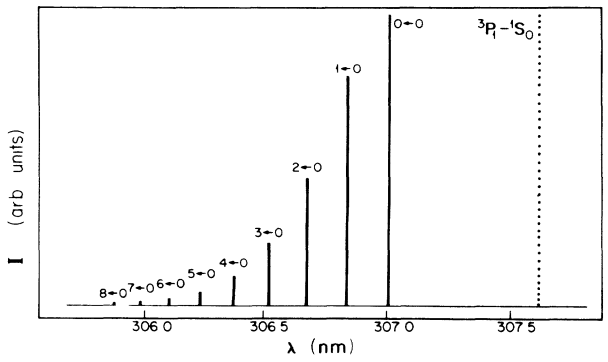

FIG. 5. Computer simulation of the $O_u^+(^3\Pi_u)\leftarrow XO_g^+(^1\Sigma_g^+)$ excitation spectrum showing relative intensities of the vibrational components.

$U(R)\approx -c/R^6$, and the interaction is of the induced dipole-induced dipole type, in which case the London dispersion forces play an important role in the molecular formation. A reasonable approximation to London's expression is given by[19]

$$U(R)=-\left[\frac{3I_1\cdot I_2}{2(I_1+I_2)}\right]\left[\frac{\alpha_1\cdot\alpha_2}{R^6}\right], \tag{6}$$

where α_1 and α_2 are the polarizabilities of the two atoms, and I_1 and I_2 are the ionization potentials (IP). Assuming $U(R)=D_e''$ as a measure of the dissociation energies, it is possible to calculate r_e'' of Hg_2, Cd_2, and Zn_2 if the IP and α values are known. Using this approach we calculated yet another set of r_e'' values, which is also included

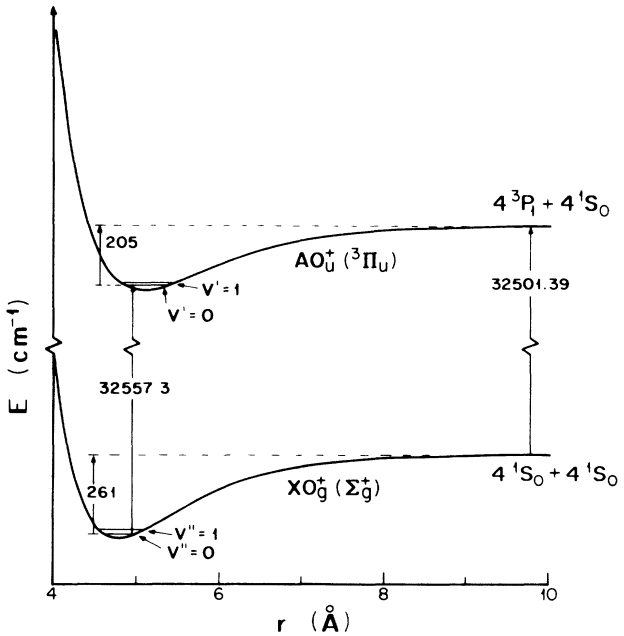

FIG. 6. A potential-energy diagram calculated from the experimental data using the Morse potential.

TABLE III. Spectroscopic constants of the $XO_g^+(^1\Sigma_g^+)$ and $O_u^+(^3\Pi_u)$ states in Hg_2, Cd_2, and Zn_2.

	Hg_2[a]		Cd_2[b]		Zn_2[c]	
Designation	XO_g^+	O_u^+	XO_g^+	O_u^+	XO_g^+	O_u^+
ω_e (cm^{-1})	18.5±0.5	19.7±0.5	23.0±0.2	18.4±0.2	25.7±0.2	20.1±0.2
$\omega_e x_e$ (cm^{-1})	0.27	0.21	0.40	0.33	0.60±0.05	0.47±0.05
D_e (cm^{-1})	350±20	410±10	323.0±0.5	252.0±0.5	274.0±0.5	215.0±0.5
n_v	~34	~47	~29	~28	~21	~21
r_e (Å)	3.63±0.04	3.61±0.5	5.10±0.07[d]	5.4±0.1[d]	4.80±0.07[d]	5.1±0.1[d]
r_e (Å)	4.5[a], 4.07[e]		4.26[e]	4.52[e]	4.67[e]	4.97[e]
	$\alpha_{Hg}=34.0(a_0^3)$[f]		$\alpha_{Cd}=40.5(a_0^3)$[f]		$\alpha_{Zn}=47.8(a_0^3)$[f]	
$r_e'-r_e''$ (Å)	−0.02±0.5	−0.02±10.5	0.26±0.03	0.26±0.03	0.30±0.03	0.30±0.03

[a]van Zee Blankespoor, and Zwier, Ref. 2.
[b]Czajkowski, Bobkowski, and Krause, Ref. 4.
[c]This work.
[d]Calculated from the Morse relation.
[e]Calculated from the London dispersion relation.
[f]Miller and Bederson, Ref. 21.

in Table III, taking the IP values from Moore,[20] the polarizabilities as recommended by Miller and Bederson,[21] and D_e'' values from Ref. 4 and from this work. The resulting value for Hg_2 is 12% larger than that determined from the analysis of the Hg_2 spectrum by van Zee, Blankespoor, and Zwier.[2]

Our belief in the correctness of our experimentally determined r_e'' values for Cd_2 and Zn_2 is reinforced by the results of the following exercise. Using the polarizabilities $\alpha_{Cd}=40.5(a_0^3)$ and $\alpha_{Ar}=11.1(a_0^3)$ from Ref. 21, and $D_e''=106.5$ cm^{-1} for the $X^1O_u^+$ state of the CdAr molecule,[22] we calculated $r_e''(X^1O_u^+)=4.30$ Å, in excellent agreement with the recently reported value $r_e''=4.33$ Å obtained from a measurement of the rotational constant B_e''.[16]

IV. CONCLUSIONS

The vibrational structure of the $O_u^+(^3\Pi_u) \leftarrow XO_g^+(^1\Sigma_g^+)$ excitation spectrum of the Zn_2 molecule was observed and analyzed for the first time, yielding the spectroscopic constants for the two states. Assuming a dipole-dipole interaction between ground-state Zn atoms and using London's relation for the interaction energy in conjunction with the experimental data, we obtained the internuclear separation r_e'' in the ground state. A computer fit of the FC factors to the molecular spectrum yielded the separation r_e' in the excited state. Further experiments on the spectroscopy of the Zn_2 molecule are in progress.

ACKNOWLEDGMENTS

The authors wish to acknowledge the contribution of Werner Grewe who fabricated the molybdenum expansion chamber. This research was supported in part by the Natural Sciences and Engineering Research Council of Canada. One of us (R.B.) received partial support from the Institute of Physics, Nicholas Copernicus University, Toruń, Poland, under Project No. CPB01.06.

*On leave from the Institute of Physics, Nicholas Copernicus University, Toruń, Poland.

[1]R. J. Niefer, J. Supronowicz, J. B. Atkinson, and L. Krause, Phys. Rev. A **35**, 4629 (1987), and references within.
[2]R. D. van Zee, S. C. Blankespoor, and T. S. Zwier, J. Chem. Phys. **88**, 4650 (1988).
[3]A. Kowalski, M. Czajkowski, and W. H. Breckenridge, Chem. Phys. Lett. **121**, 217 (1985).
[4]M. Czajkowski, R. Bobkowski, and L. Krause, Phys. Rev. A **40**, 4338 (1989).
[5]W. Kedzierski, J. B. Atkinson, and L. Krause, Optics Lett. **14**, 607 (1989).
[6]T. Efthimiopoulos, B. P. Stoicheff, and R. I. Thompson, Opt. Lett. **14**, 624 (1989).
[7]K. Fuke, T. Saito, H. Hiroguchi, S. Tsuchiya, K. Yamanouchi, J. Fukuyama, and K. Kaya, J. Chem. Phys. **85**, 1806 (1986).
[8]C. Jouvet and B. Soep, J. Chem. Phys. **80**, 2229 (1984).
[9]A. Zehnacker, M. C. Duval, C. Lardeux-Dedonder, D. Solgadi, B. Soep, and O. Benoit d'Azy, J. Chem. Phys. **86**, 6565 (1987).
[10]K. Fuke, T. Saito, and K. Kaya, J. Chem. Phys. **79**, 2487 (1983).
[11]S. Mocarski (private communication).
[12]J. R. Nestor, Appl. Opt. **21**, 4554 (1982).
[13]W. Kedzierski, R. Berends, J. B. Atkinson, and L. Krause, J. Phys. E **21**, 796 (1988).
[14]C. F. Bender, T. N. Rescigno, H. F. Schaefer, and A. E. Orel, J. Chem. Phys. **71**, 1122 (1979).
[15]P. J. Hay, T. H. Dunning, and R. C. Raffenetti, J. Chem. Phys. **65**, 2679 (1976).
[16]A. Kvaran, D. J. Funk, A. Kowalski, and W. H. Breckenridge, J. Chem. Phys. **89**, 6069 (1988).
[17]D. M. Lubman, C. T. Rettner, and R. N. Zare, J. Chem. Phys.

86, 1129 (1982).
[18]P. M. Morse, Phys. Rev. **34**, 57 (1929).
[19]F. London, Z. Phys. **63**, 243 (1930); Z. Phys. Chem. B **11**, 222 (1930).
[20]Charlotte E. Moore, *Atomic Energy Levels*, Natl. Bur. Stand. Ref. Data Ser., Natl. Bur. Stand. (U.S.) Circ. No. 35 (U.S. GPO, Washington, D. C., 1971), Vols. 2 and 3.
[21]T. M. Miller and B. Bederson, in *Advances in Atomic and Molecular Physics*, edited by D. R. Bates and B. Bederson (Academic, New York, 1977), Vol. 13, p. 1.
[22]R. Bobkowski, M. Czajkowski, and L. Krause, Phys. Rev. A **41**, 243 (1990).